

Discovery potential of a long-lived partner of inelastic dark matter at MATHUSLA in $U(1)_{X_3}$ extension of the standard model

Nobuchika Okada^{*}

Department of Physics and Astronomy,

University of Alabama, Tuscaloosa, Alabama 35487, USA

Osamu Seto[†]

Department of Physics, Hokkaido University, Sapporo 060-0810, Japan

Abstract

We investigate the discovery potential at the MATHUSLA experiment of a long-lived particle (LLP), which is the heavier state of inelastic scalar dark matter (DM) in third generation-philic $U(1)$ ($U(1)_{X_3}$) extension of the standard model. Since the heavier state and DM state form the complex scalar charged under the $U(1)_{X_3}$, it is natural that the heavier state P is almost degenerate with the DM state and hence long-lived. We find that third generation-philic right-handed $U(1)$, $U(1)_{R_3}$, model is the most interesting, because third generation-philic models are less constrained by the current experimental results and right-handed $U(1)$ interactions leave visible final decay products without producing neutrinos. For a benchmark of the model parameters consistent with the current phenomenological constraints, we find that the travel distance of the LLP can be $\mathcal{O}(100)$ m and the LLP production cross section at the 14 TeV LHC can be $\mathcal{O}(10)$ fb. Thus, we conclude that the LLP can be discovered at the MATHUSLA with a sufficiently large number of LLP decay events inside the MATHUSLA detector.

^{*}Electronic address: okadan@ua.edu

[†]Electronic address: seto@particle.sci.hokudai.ac.jp

I. INTRODUCTION

Explanation of the neutrino oscillation phenomena between neutrino flavor species due to non-zero neutrino mass and existence of dark matter (DM) in the Universe require undiscovered particles and interactions of beyond the standard model (BSM) of particle physics. Nevertheless, any evidence of new particles in BSM have not yet been reported in any ongoing experiments. A reason of non-discovery of a new particle might be due to not its large mass but its extremely weak interaction strength, in other words, a relevant coupling constant is very small. Even if coupling constants and hence the resultant production cross sections of new particles are very small, we may expect certain amount of production of new particles if experiments are conducted with huge luminosity. The small coupling constant makes the new particle long-lived, and signals of such long-lived particles (LLPs), if they are electrically neutral, would be discovered through their “displaced vertex” signatures. In fact, displaced vertex signatures have been searched for at, for instance, ATLAS [1] and FASER [2] in Large Hadron Collider (LHC). Some near-future experiments such as FASER2 [3] will start soon, and other several future experiments have been proposed, targeting various range of LLP masses and decay lengths. Among such proposed future experiments for the displaced vertex search, MAssive Timing Hodoscope for Ultra Stable neutralL pArticles (MATHUSLA) experiment is striking, because it will be able to search LLPs with the decay length of the order of 100 m [4]. Theoretical studies on search sensitivity for various BSM models have been examined in Refs. [5–40].

The null results in dark matter direct detection experiments constrain models of Weakly Interacting Massive Particles (WIMPs) DM [41]. The null results in indirect searches of DM also constrain the present DM annihilation cross section and exclude WIMPs annihilating into $b\bar{b}$ quarks in s-wave processes with the cross section of about $3 \times 10^{-26} \text{ cm}^3/\text{s}$, which is the typical value for thermal WIMPs, with mass up to a few hundreds of GeV [42, 43]. Despite such stringent constraints, there are still many viable WIMP models. One of those model proposed in Ref. [44] is an extra $U(1)$ interacting scalar inelastic dark matter, which is consistent with null results of direct DM searches due to its inelastic nature [45, 46] and of indirect DM search because thermal abundance in the early Universe is fixed by coannihilation cross section [47, 48] rather than the self-annihilation cross section [49].

In the models of Ref. [44], both DM state and the heavier state relevant for both co-

annihilation and inelastic scattering of DM state originate from one complex scalar field. Since they belong to the single complex scalar field, those two states are naturally well degenerate. The decay rate of the heavier state into the lighter one (DM state) would be very small due to its very small phase space volume, so that the heavier state could be a natural candidate for the LLP that we are interested in. To examine the MATHUSLA prospects, inelastic DM models have been proposed [12, 23, 27]¹. While the longevity of LLP in fermionic inelastic DM model proposed in Ref. [12] is due to the mass degeneracy as well as its tiny kinetic mixing of dark photon, the LLP in our scalar inelastic DM model is long-lived due to only about 1% mass degeneracy.

This paper is organized as follows: In Sec. II, we describe the extra gauge $U(1)$ interacting inelastic model, which is a variant of the original models in Ref. [44]. We identify a parameter set to reproduce thermal DM abundance and a benchmark point in Sec. III. In Sec. IV, for the benchmark point, we present a search prospect of LLPs by the MATHUSLA experiment. Section V is devoted to our summary.

II. THE MODEL

There are several possibilities of anomaly free gauged $U(1)$ extension of the standard model. Among them, the best studied model is the flavor universal $U(1)_{B-L}$ [50–53]. However, because the new neutral gauge boson Z' in the $U(1)_{B-L}$ model interacts with the first and the second generation of SM fermions, the experimental constraints on the couplings are very stringent [54–56]. Thus, we may not expect a sizable production cross section for the LLP production from the Z' boson decay. Note that anomaly cancellation of $U(1)_{B-L}$ model is realized in each generation of fermions, hence it is generally possible for only a particular generation to be charged under the $U(1)$. The model where only the third generation fermions are charged, $U(1)_{(B-L)_3}$, is such a choice [44, 57–60] and well studied. As expected, the experimental constraints on the $U(1)_{(B-L)_3}$ model are much weaker compared with the universal $U(1)_{B-L}$ model [61–65]. It is easy to generalize the $U(1)_{B-L}$ model to the $U(1)_X$ model by assigning the $U(1)$ charge for a field as a linear combination of its $U(1)_Y$ and $U(1)_{B-L}$ charge. Since $U(1)_Y$ and $U(1)_{B-L}$ are independently anomaly free, the $U(1)_X$

¹ The mass splitting in Refs. [23, 27] is generated by an explicit gauge symmetry breaking term, and models have not been formulated in gauge invariant manner.

	SU(3) _c	SU(2) _L	U(1) _Y	U(1) _{X₃}
Q^i	3	2	1/6	$(\frac{1}{6}x_H + \frac{1}{3})\delta_{i3}$
u_R^i	3	1	2/3	$(\frac{2}{3}x_H + \frac{1}{3})\delta_{i3}$
d_R^i	3	1	-1/3	$(-\frac{1}{3}x_H + \frac{1}{3})\delta_{i3}$
L^i	1	2	-1/2	$(-\frac{1}{2}x_H - 1)\delta_{i3}$
e_R^i	1	1	-1	$(-x_H - 1)\delta_{i3}$
Φ	1	2	1/2	$\frac{1}{2}x_H$
N_R^i	1	1	0	$-\delta_{i3}$
ϕ_1	1	1	0	+1
ϕ_2	1	1	0	+2

TABLE I: The particle contents of our $U(1)_{X_3}$ model. In addition to the SM particle content ($i = 1, 2, 3$), three RH neutrinos (N_R^i ($i = 1, 2, 3$)) and two $U(1)_{X_3}$ scalar fields (ϕ_1 and ϕ_2) are introduced. The scalar ϕ_2 is the Higgs field and develops its VEV to break the $U(1)_{X_3}$ symmetry, while ϕ_1 has no VEV and includes the inelastic DM and its partner LLP as its components.

is automatically anomaly free [66–68]. A special case is so-called $U(1)_R$ model, where only right-handed (RH) SM fermions and RH neutrinos are charged under the $U(1)$ [69]. In this paper, we generalize $U(1)_{(B-L)_3}$ to $U(1)_{X_3}$, where X_3 denotes a linear combination of $U(1)_{Y_3}$ and $U(1)_{(B-L)_3}$. We introduce an $U(1)_{X_3}$ charged scalar field ϕ_1 with its charge +1 in addition to the minimal particle contents. The total particle contents are listed in Tab. I. The field ϕ_2 is responsible to break $U(1)_{X_3}$ gauge symmetry and x_H is a real parameter which parameterize a combination weight of $(B - L)_3$ and Y_3 .

The $U(1)_{X_3}$ gauge interaction for an SM chiral fermion and RH neutrinos ($f_{L/R}$) can be read from the usual covariant derivative,

$$\mathcal{L}_{\text{int}} = \sum_{f_j} \overline{f_j} \gamma^\mu X_\mu g_{X_3} (q_{f_j L} P_L + q_{f_j R} P_R) f_j, \quad (1)$$

where X^μ is the $U(1)_{X_3}$ gauge field, g_{X_3} is the gauge coupling constant, and $q_{f_j L/R}$ is a $U(1)_{X_3}$ charge of $f_{jL/R}$ (see Tab. I).

The scalar potential, which is gauge-invariant and renormalizable, is expressed as [70, 71]

$$\begin{aligned} V(\Phi, \phi_1, \phi_2) = & -M_\Phi^2 |\Phi|^2 + \frac{\lambda}{2} |\Phi|^4 + M_{\phi_1}^2 \phi_1 \phi_1^\dagger - M_{\phi_2}^2 \phi_2 \phi_2^\dagger \\ & + \frac{1}{2} \lambda_1 (\phi_1 \phi_1^\dagger)^2 + \frac{1}{2} \lambda_2 (\phi_2 \phi_2^\dagger)^2 + \lambda_3 \phi_1 \phi_1^\dagger (\phi_2 \phi_2^\dagger) \\ & + (\lambda_4 \phi_1 \phi_1^\dagger + \lambda_5 \phi_2 \phi_2^\dagger) |\Phi|^2 - A (\phi_1 \phi_1 \phi_2^\dagger + \phi_1^\dagger \phi_1^\dagger \phi_2), \end{aligned} \quad (2)$$

with Φ being the SM Higgs doublet field. All parameters, M_i^2 , λ_i and A , in the potential (2) are taken to be real and positive.

A. Dark matter mass and interactions

At the $U(1)_{X_3}$ and the electroweak (EW) symmetry breaking vacuum, the SM Higgs field and the $U(1)$ Higgs field are expanded around those VEVs, v and v_2 , as (in the unitary gauge)

$$\Phi = \begin{pmatrix} 0 \\ \frac{v+\varphi}{\sqrt{2}} \end{pmatrix}, \quad (3)$$

$$\phi_1 = \frac{S + iP}{\sqrt{2}}, \quad (4)$$

$$\phi_2 = \frac{v_2 + \varphi_2}{\sqrt{2}}. \quad (5)$$

The physical states (φ and φ_2) are diagonalized to the mass eigenstates (h and H) with masses m_h and m_H as

$$\begin{pmatrix} \varphi \\ \varphi_2 \end{pmatrix} = \begin{pmatrix} \cos \alpha & \sin \alpha \\ -\sin \alpha & \cos \alpha \end{pmatrix} \begin{pmatrix} h \\ H \end{pmatrix}. \quad (6)$$

For a small mixing angle α , h is identified with the SM-like Higgs boson. Hereafter, we set α negligibly small. With the $U(1)_{X_3}$ and the EW symmetry breaking, the Z' boson which is the mass eigenstate after the X becomes massive, S and P acquire their masses, respectively, as

$$m_{Z'}^2 = g_{X_3}^2 4v_2^2, \quad (7)$$

$$m_S^2 = M_{\phi_1}^2 + \frac{1}{2} \lambda_3 v_2^2 + \frac{1}{2} \lambda_4 v^2 - \sqrt{2} A v_2, \quad (8)$$

$$m_P^2 = M_{\phi_1}^2 + \frac{1}{2} \lambda_3 v_2^2 + \frac{1}{2} \lambda_4 v^2 + \sqrt{2} A v_2. \quad (9)$$

Note that the parameter A controls the mass splitting between S and P . Since we take A positive, S is lighter than P and becomes the DM candidate. The other choice of $A < 0$ causes no essential difference in our final results, except that P is the DM particle in the case.

Gauge interaction of the DM particle is expressed as

$$\mathcal{L}_{\text{int}} = g_{X_3} Z'^\mu ((\partial_\mu S) P - S \partial_\mu P), \quad (10)$$

and similarly 3rd generation quarks and leptons also interact with Z' boson with corresponding charges. The absence of Z' -DM-DM coupling indicates that the Z' -mediating DM scattering off with a nucleon is inelastic and ineffective for a mass splitting larger than the maximal energy transfer in the scatterings [45, 46]. Elastic scattering through Higgs bosons exchange [72] can be neglected since we have set a very small Higgs mixing α . We also set the coupling constant A very small, so that S and P are well degenerate in mass. This degeneracy is crucial not only for the scalar P being long-lived, but also for reproducing the observed DM relic density through S and P coannihilation process.

B. The decay width of Z' boson

The partial decay width of $Z' \rightarrow f\bar{f}$ is given by

$$\Gamma(Z' \rightarrow f\bar{f}) = \frac{1}{48\pi m_{Z'}^2} N_c |\mathcal{M}|^2 \sqrt{m_{Z'}^2 - 4m_f^2}, \quad (11)$$

$$|\mathcal{M}|^2 = 2g_{X_3}^2 (q_{fL}^2 (m_{Z'}^2 - m_f^2) + 6q_{fL}q_{fR}m_f^2 + q_{fR}^2 (m_{Z'}^2 - m_f^2)), \quad (12)$$

where the number of color N_c is 3 for quarks and 1 for leptons. If $m_f \ll m_{Z'}$, then Eq. (11) is reduced to

$$\Gamma(Z' \rightarrow f\bar{f}) \simeq \frac{g_{X_3}^2 N_c m_{Z'}}{24\pi} (q_{fL}^2 + q_{fR}^2). \quad (13)$$

We obtain the partial decay width of Z' into S and P as

$$\Gamma(Z' \rightarrow SP) = \frac{g_{X_3}^2}{48\pi} \frac{(m_{Z'}^2 - (m_P - m_S)^2)^{3/2} (m_{Z'}^2 - (m_P + m_S)^2)^{3/2}}{m_{Z'}^5}, \quad (14)$$

from the vertex (10). The decay branching ratios are shown in Fig. 1. Note that $Br(Z' \rightarrow \nu_\tau \nu_\tau)$ vanishes at $x_H = -2$, which corresponds to $U(1)$ right-handed, $U(1)_R$. This fact plays an important role in the following discussion.

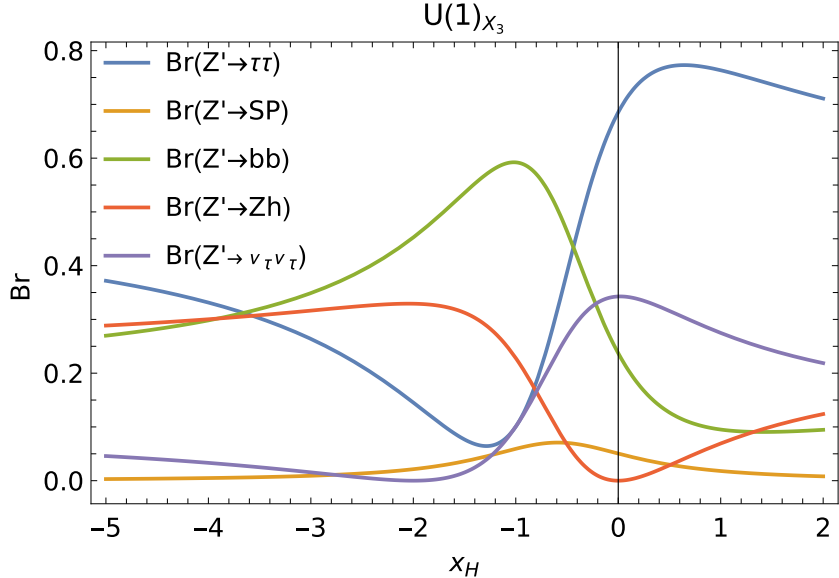


FIG. 1: Branching ratios of the Z' decay for $g_X = 0.1$, $m_S = 130$ GeV and $m_{Z'} = 350$ GeV.

C. Decay of P

If S and P are strongly degenerate so that the mass difference is much smaller than the mass of Z' , the two body decay of P is kinematically forbidden. Thus, for the main decay mode, $P \rightarrow SZ'^* \rightarrow Sff\bar{f}$, the total decay width (Γ), or equivalently the inverse of the lifetime (τ),

$$\Gamma = \frac{1}{\tau} = \frac{1}{2p^0} \int \overline{|\mathcal{M}(P \rightarrow Sff\bar{f})|^2} dQ, \quad (15)$$

is suppressed by the phase space volume [73]. As a result, P is short-lived in cosmology but can be long-lived in collider experiments. The expected travel distance $c\tau$ for $x_H = -2$, in other words $U(1)_{R_3}$, is shown as the function of its mass m_P in Fig. 2. We note that the mass difference,

$$m_P^2 - m_S^2 = 2\sqrt{2}Av_2, \quad (16)$$

from Eqs. (8) and (9), is always adjustable by suitably choosing the free parameter A such that $c\tau$ becomes about 100 m, which is ideal for the detection of P decay inside the MATHUSLA detector. Here and hereafter, we have focused on the $U(1)_{R_3}$ case. For $x_H \neq -2$, the decay mode of $P \rightarrow SZ'^* \rightarrow S\nu_\tau\nu_\tau$ exists and becomes the dominant mode for $M_P - m_S \leq 2m_\tau$. In this case, the LPP P provides only invisible decay products.

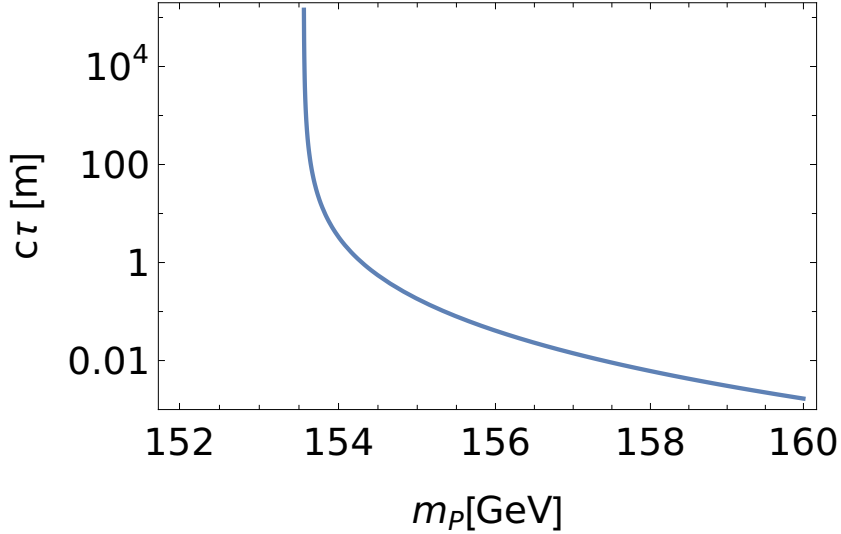


FIG. 2: $c\tau$ for $g_{R_3} = 0.1$, $m_S = 150$ GeV and $m_{Z'} = 350$ GeV. Near the threshold $m_P - m_S \simeq 2m_\tau$ with m_τ being the tau-lepton mass, $c\tau$ is very long.

III. DARK MATTER AND LHC CONSTRAINTS

For evaluation of prospect at MATHUSLA in the next section, in this section, we will find a benchmark point which satisfies the thermal DM abundance and the latest LHC constraints. As mentioned above, we concentrate on the $U(1)_{R_3}$ model. The LLP P in other general $U(1)_{X_3}$ ($x_H \neq -2$) may decay into neutrinos which are invisible for the MATHUSLA detector. Thus, the $U(1)_{R_3}$ model is the best choice from the viewpoint of the detection with a large decay length of $\mathcal{O}(100)$ m.

A. Thermal relic abundance

We estimate the thermal relic abundance of the real scalar DM, S , by solving the Boltzmann equation,

$$\frac{dn}{dt} + 3Hn = -\langle\sigma_{\text{eff}}v\rangle(n^2 - n_{\text{EQ}}^2), \quad (17)$$

where H and n_{EQ} are the Hubble parameter and the DM number density at thermal equilibrium, respectively [49]. In our model, the main annihilation mode is coannihilation $SP \rightarrow f\bar{f}$ through s -channel Z' exchange for $m_{Z'} > m_S$ and the annihilation mode $SS \rightarrow Z'Z'$ by $u(t)$ -channel P exchange for $m_{Z'} < m_S$ [44]. We use the effective thermal averaged annihilation

cross section

$$\langle \sigma_{\text{eff}} v \rangle = \sum_{i,j=S,P} \langle \sigma_{ij} v_{ij} \rangle \frac{n_i}{n_{\text{EQ}}} \frac{n_j}{n_{\text{EQ}}}, \quad (18)$$

to include the coannihilation effects properly and n in Eq. (17) should be understood as $n = \sum_i n_i$ for $i = S, P$ [47, 48]. The contours of thermal DM abundance $\Omega h^2 \simeq 0.1$ [74] (blue curve) and $\text{Br}(Z' \rightarrow SP)$ (green curves) for the $U(1)_{R_3}$ model are shown in Fig. 3.

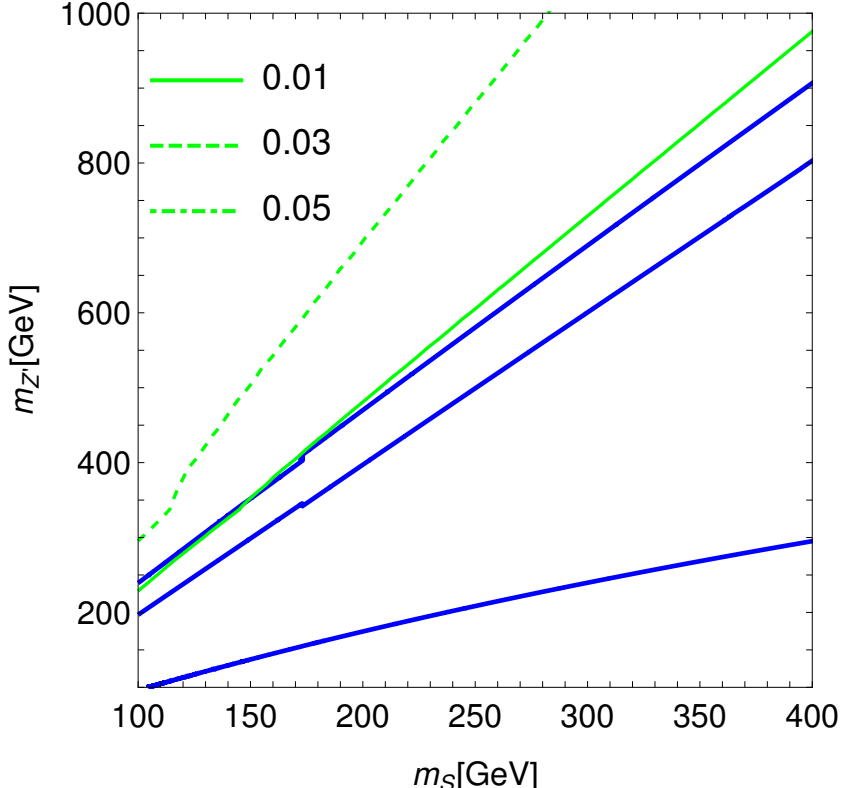


FIG. 3: The contour (in blue) along which the observed DM relic abundance $\Omega h^2 \simeq 0.1$ is reproduced for $g_{R_3} = 0.1$ and $x_H = -2$.

B. Benchmark points

To find a viable benchmark point, we also take the Z' boson search at the LHC with ditau final state [75, 76] into account. We evaluate the production cross section for the process $pp \rightarrow \tau^+ \tau^-$ given by

$$\sigma(pp \rightarrow Z') \text{BR}(Z' \rightarrow \tau^+ \tau^-), \quad (19)$$

where the branching ratio is calculated from Eq. (11). As can be seen in Eq. (12), $\text{BR}(Z' \rightarrow \tau^+ \tau^-)$ depends on the value of x_H , and we focus on $x_H = -2$ as stated above.

With the decay rates of X estimated in Sec. II B, as in Ref. [56], since the total X boson decay width is very narrow, we use the narrow width approximation to evaluate the X boson production cross section

$$\sigma(pp \rightarrow X) = 2 \sum_{q,\bar{q}} \int dx \int dy f_q(x, Q) f_{\bar{q}}(x, Q) \hat{\sigma}(\hat{s}), \quad (20)$$

$$\hat{\sigma}(\hat{s}) = \frac{4\pi^2}{3} \frac{\Gamma_X(X \rightarrow q\bar{q})}{m_X} \delta(\hat{s} - m_X^2), \quad (21)$$

where f_q and $f_{\bar{q}}$ are the parton distribution function (PDF) for a quark and antiquark (b and \bar{b} in our model), $\hat{s} = x y s$ is the invariant mass squared of colliding quarks for the center of mass energy s . The factor 2 in Eq. (20) counts two ways of q coming from which proton out of two colliding protons. Since the most severe bound is from the dilepton channel ($\ell = \tau$), we calculate $\sigma(pp \rightarrow X) \text{Br}(X \rightarrow \tau^+ \tau^-)$ and compare it with the CMS results [75]². We employ PDFs of CTEQ6L [77] with a factorization scale $Q = m_{Z'}$ for simplicity.

The resultant production cross section is shown in the second column in Tab. III. The production cross section is consistent with and smaller than the latest most stringent bound from the CMS [75] at the LHC. We summarize parameters and masses of relevant particles in Tab. II.

	x_H	g_{X_3}	$m_{Z'}$	m_S
BP_{-2}	-2	0.1	351 GeV	150 GeV

TABLE II:

IV. PROSPECT FOR MATHUSLA

The travel distance $c\tau \simeq 100$ m is the most sensitive range at MATHUSLA [4, 78, 79]. The pair production cross section of such a LLP χ for its 5σ discovery can be read as $\sigma_{\chi\chi} > 0.3$ fb from Fig. 1 in Ref. [9]. On the other hand, in our scenario, the LLP P is not pair produced but singly produced through $pp \rightarrow Z' \rightarrow SP$. Thus, the required production

² The ATLAS bound [76] is somewhat weaker than that from the CMS.

	$\sigma(pp \rightarrow Z' \rightarrow \tau\tau)$ (CMS bound on it)	σ_{SP} @13TeV LHC	σ_{SP} @14TeV LHC
BP_{-2}	154 fb (< 203 fb)	10.8 fb	12.9 fb

TABLE III:

cross section for the LLP P to be discovered at the MATHUSLA would be set to be larger than 0.6 fb. In Tab. III, we list the SP production cross section at 13 TeV LHC and 14 TeV LHC for our benchmark on Tab. II satisfying the DM abundance and the LHC bounds. We find that the MATHUSLA will be able to discover those LLPs because the production cross section σ_{SP} is sufficiently larger than 0.6 fb.

V. SUMMARY

We have proposed a simple extension of the SM with an extra $U(1)_{R_3}$ gauge interaction with scalar particle of DM candidate with the charge 1, third generation of SM fermions and third generation of right-handed neutrinos. After the SM singlet $U(1)_{R_3}$ breaking scalar with the charge 2 develops the VEV, the gauge boson acquires the mass, and the tiny mass splitting between real and imaginary component of the charge 1 scalar appears through the scalar tri-linear interaction. The lighter scalar S is inelastic DM candidate with the heavier state P . Due to the mass degeneracy, the slightly heavier state P is long-lived and will be able to be discovered as LLPs.

We have calculated the production cross section of LLP P through the process $pp \rightarrow Z' \rightarrow SP$ at the MATHUSLA for a benchmark point which satisfies stringent LHC bounds and thermal DM abundance. The production cross section of benchmark point turns out to be about 10 fb, which is about an order of magnitude larger than the cross section required by 5σ discovery as a LLP at the MATHUSLA. Thus, we conclude that the heavier state of inelastic DM in our model can be discovered at the MATHUSLA.

Acknowledgments

This work is supported in part by the U.S. DOE Grant No. DE-SC0012447 and DE-SC0023713 (N.O.) and KAKENHI Grants No. JP23K03402 (O.S.).

Appendix A: The decay rate of P

The spin averaged squared amplitude for $P(p) \rightarrow f(q_1)\bar{f}(q_2)S(q_3)$ is given by

$$\begin{aligned}
& \overline{|\mathcal{M}|^2} \\
&= \frac{2g_{R_3}^4}{m_{Z'}^4 (-2(p \cdot q_3) + m_P^2 + m_S^2 - m_{Z'}^2)^2} \left(-2(-m_P^2 + m_S^2 + m_{Z'}^2)^2 (p \cdot q_1)^2 \right. \\
&\quad - 2(m_P^2 - m_S^2 + m_{Z'}^2)^2 (q_1 \cdot q_3)^2 + 4 \left((m_P^2 - m_S^2)^2 - m_{Z'}^4 \right) (p \cdot q_1) (q_1 \cdot q_3) \\
&\quad - 2(-m_P^2 + m_S^2 + m_{Z'}^2)^2 (p \cdot q_1) (p \cdot q_3) + 2(m_P^2 - m_S^2 + m_{Z'}^2)^2 (q_1 \cdot q_3) (p \cdot q_3) \\
&\quad + m_f^2 \left(-2 \left((m_P^2 - m_S^2)^2 - m_{Z'}^4 \right) (p \cdot q_3) + m_{Z'}^4 (m_P^2 + m_S^2) + (m_P^2 - m_S^2)^2 (m_P^2 + m_S^2 - 2m_{Z'}^2) \right) \\
&\quad + (p \cdot q_1) \left(m_{Z'}^4 (m_P^2 - 3m_S^2) + 2m_{Z'}^2 (m_S^4 - m_P^4) + (m_P^2 - m_S^2)^2 (m_P^2 + m_S^2) \right) \\
&\quad \left. + (q_1 \cdot q_3) \left(m_P^4 (m_S^2 - 2m_{Z'}^2) + m_P^2 (m_S^4 + 3m_{Z'}^4) - m_P^6 - (m_S^3 - m_S m_{Z'}^2)^2 \right) \right). \quad (A1)
\end{aligned}$$

The integration of phase space volume is reduced to

$$\begin{aligned}
dQ &= \frac{d^3 q_1}{(2\pi)^3 2q_1^0} \frac{d^3 q_2}{(2\pi)^3 2q_2^0} \frac{d^3 q_3}{(2\pi)^3 2q_3^0} (2\pi)^4 \delta^{(4)}(p - q_1 - q_2 - q_3) \\
&= \frac{1}{(2\pi)^5} \frac{d^3 q_1}{2q_1^0} \frac{d^3 q_3}{2q_3^0} \delta \left((m_P - q_1^0 - q_3^0)^2 - (|\mathbf{q}_1|^2 + |\mathbf{q}_3|^2) - 2|\mathbf{q}_1||\mathbf{q}_3| \cos \theta_{13} - m_f^2 \right) \\
&= \frac{1}{8(2\pi)^5} dq_1^0 dq_3^0 d\Omega_1 d\varphi_{13} d\cos \theta_{13} \delta \left(\frac{(m_P - q_1^0 - q_3^0)^2 - |\mathbf{q}_1|^2 - |\mathbf{q}_3|^2 - m_f^2}{2|\mathbf{q}_1||\mathbf{q}_3|} - \cos \theta_{13} \right). \quad (A2)
\end{aligned}$$

Then, the integration range of energy turns out to be

$$q_3^{\min}(q_1^0) < q_3^0 < q_3^{\max}(q_1^0), \quad (A3)$$

with

$$q_3^{\min}(q_1^0) = \frac{(m_P - q_1^0)(m_P^2 - 2m_P q_1^0 + m_S^2) - \sqrt{\left((q_1^0)^2 - m_f^2 \right) \left((m_P^2 - 2m_P q_1^0 - m_S^2)^2 - 4m_f^2 m_S^2 \right)}}{2(m_f^2 + m_P(m_P - 2q_1^0))}, \quad (A4)$$

$$q_3^{\max}(q_1^0) = \frac{(m_P - q_1^0)(m_P^2 - 2m_P q_1^0 + m_S^2) + \sqrt{\left((q_1^0)^2 - m_f^2 \right) \left((m_P^2 - 2m_P q_1^0 - m_S^2)^2 - 4m_f^2 m_S^2 \right)}}{2(m_f^2 + m_P(m_P - 2q_1^0))}, \quad (A5)$$

and

$$m_f < q_1^0 < \frac{m_P^2 - m_S^2 - 2m_f m_S}{2m_P}. \quad (\text{A6})$$

By integrating the differential decay rate

$$d\Gamma = \frac{1}{2p^0} \overline{|\mathcal{M}|^2} dQ = \frac{1}{8(2\pi)^3 m_P} \left[\overline{|\mathcal{M}|^2} \delta(\dots - \cos \theta_{13}) d\cos \theta_{13} \right] dq_1^0 dq_3^0, \quad (\text{A7})$$

for the range (A3) and (A6), we obtain the travel distance shown in Fig. 2.

[1] G. Aad *et al.* [ATLAS], JHEP **2306**, 158 (2023).

[2] H. Abreu *et al.* [FASER], Phys. Lett. B **848**, 138378 (2024).

[3] A. Ariga *et al.* [FASER], Phys. Rev. D **99**, no.9, 095011 (2019).

[4] J. P. Chou, D. Curtin and H. J. Lubatti, Phys. Lett. B **767**, 29-36 (2017).

[5] P. S. Bhupal Dev, R. N. Mohapatra and Y. Zhang, Phys. Rev. D **95**, no.11, 115001 (2017).

[6] J. A. Evans, Phys. Rev. D **97**, no.5, 055046 (2018).

[7] J. C. Helo, M. Hirsch and Z. S. Wang, JHEP **07**, 056 (2018).

[8] F. F. Deppisch, W. Liu and M. Mitra, JHEP **08**, 181 (2018).

[9] S. Jana, N. Okada and D. Raut, Phys. Rev. D **98**, no.3, 035023 (2018).

[10] M. Bauer, M. Heiles, M. Neubert and A. Thamm, Eur. Phys. J. C **79**, no.1, 74 (2019).

[11] D. Curtin, K. R. Dienes and B. Thomas, Phys. Rev. D **98**, no.11, 115005 (2018).

[12] A. Berlin and F. Kling, Phys. Rev. D **99**, no.1, 015021 (2019).

[13] D. Derckx, J. De Vries, H. K. Dreiner and Z. S. Wang, Phys. Rev. D **99**, no.5, 055039 (2019).

[14] F. Deppisch, S. Kulkarni and W. Liu, Phys. Rev. D **100**, no.3, 035005 (2019).

[15] J. M. No, P. Tunney and B. Zaldivar, JHEP **03**, 022 (2020).

[16] Z. S. Wang and K. Wang, Phys. Rev. D **101**, no.7, 075046 (2020).

[17] K. Jodłowski, F. Kling, L. Roszkowski and S. Trojanowski, Phys. Rev. D **101**, no.9, 095020 (2020).

[18] P. D. Bolton, F. F. Deppisch and P. S. Bhupal Dev, JHEP **03**, 170 (2020).

[19] M. Hirsch and Z. S. Wang, Phys. Rev. D **101**, no.5, 055034 (2020).

[20] S. Jana, N. Okada and D. Raut, Eur. Phys. J. C **82**, no.10, 927 (2022).

[21] J. Gehrlein and S. Ipek, JHEP **05**, 020 (2021).

- [22] C. Sen, P. Bandyopadhyay, S. Dutta and A. KT, Eur. Phys. J. C **82**, no.3, 230 (2022).
- [23] J. Guo, Y. He, J. Liu and X. P. Wang, JHEP **04**, 024 (2022).
- [24] B. Bhattacherjee, S. Matsumoto and R. Sengupta, Phys. Rev. D **106**, no.9, 095018 (2022).
- [25] M. Du, R. Fang, Z. Liu and V. Q. Tran, Phys. Rev. D **105**, no.5, 055012 (2022).
- [26] A. Kamada and T. Kuwahara, JHEP **03**, 176 (2022).
- [27] E. Bertuzzo, A. Scaffidi and M. Taoso, JHEP **08**, 100 (2022).
- [28] W. Liu, J. Li, J. Li and H. Sun, Phys. Rev. D **106**, no.1, 015019 (2022).
- [29] P. Bandyopadhyay, E. J. Chun and C. Sen, JHEP **02**, 103 (2023).
- [30] Y. n. Mao, K. Wang and Z. S. Wang, Phys. Rev. D **108**, no.9, 095025 (2023).
- [31] K. Jodłowski, Phys. Rev. D **108**, no.11, 11 (2023).
- [32] P. J. Fitzpatrick, Y. Hochberg, E. Kuflik, R. Ovadia and Y. Soreq, Phys. Rev. D **108**, no.7, 075003 (2023).
- [33] D. Curtin and J. S. Grewal, Phys. Rev. D **109**, no.7, 075017 (2024).
- [34] A. Batz, T. Cohen, D. Curtin, C. Gemmell and G. D. Kribs, JHEP **04**, 070 (2024).
- [35] F. F. Deppisch, S. Kulkarni and W. Liu, [arXiv:2311.01719 [hep-ph]].
- [36] N. Bernal, K. Deka and M. Losada, Phys. Rev. D **110**, no.5, 055011 (2024).
- [37] F. Bishara, F. Sala and K. Schmidt-Hoberg, [arXiv:2401.12278 [hep-ph]].
- [38] W. Liu, L. Wang and Y. Zhang, Phys. Rev. D **110**, no.1, 015016 (2024).
- [39] J. de Vries, H. K. Dreiner, J. Groot, J. Y. Günther and Z. S. Wang, [arXiv:2406.15091 [hep-ph]].
- [40] S. Liebersbach, P. Sandick, A. Shiferaw and Y. Zhao, [arXiv:2408.07756 [hep-ph]].
- [41] E. Aprile *et al.* [XENON], Phys. Rev. Lett. **131**, no.4, 041003 (2023).
- [42] A. Cuoco, M. Krämer and M. Korsmeier, Phys. Rev. Lett. **118**, no.19, 191102 (2017).
- [43] A. McDaniel, M. Ajello, C. M. Karwin, M. Di Mauro, A. Drlica-Wagner and M. A. Sánchez-Conde, Phys. Rev. D **109**, no.6, 063024 (2024).
- [44] N. Okada and O. Seto, Phys. Rev. D **101**, no.2, 023522 (2020).
- [45] L. J. Hall, T. Moroi and H. Murayama, Phys. Lett. B **424**, 305 (1998).
- [46] D. Tucker-Smith and N. Weiner, Phys. Rev. D **64**, 043502 (2001).
- [47] K. Griest and D. Seckel, Phys. Rev. D **43**, 3191 (1991).
- [48] J. Edsjo and P. Gondolo, Phys. Rev. D **56**, 1879 (1997).
- [49] E. W. Kolb and M. S. Turner, *The Early Universe*, Addison-Wesley (1990).

[50] J. C. Pati and A. Salam, Phys. Rev. D **8**, 1240-1251 (1973).

[51] A. Davidson, Phys. Rev. D **20**, 776 (1979).

[52] R. N. Mohapatra and R. E. Marshak, Phys. Rev. Lett. **44**, 1316 (1980) [Erratum-ibid. **44**, 1643 (1980)].

[53] R. E. Marshak and R. N. Mohapatra, Phys. Lett. B **91**, 222 (1980).

[54] M. Carena, A. Daleo, B. A. Dobrescu and T. M. P. Tait, Phys. Rev. D **70**, 093009 (2004).

[55] S. Amrit, J. M. Butterworth, F. F. Deppisch, W. Liu, A. Varma and D. Yallup, JHEP **1905**, 154 (2019).

[56] A. Das, P. S. B. Dev and N. Okada, Phys. Lett. B **799**, 135052 (2019).

[57] K. S. Babu, A. Friedland, P. A. N. Machado and I. Mocioiu, JHEP **1712**, 096 (2017).

[58] R. Alonso, P. Cox, C. Han and T. T. Yanagida, Phys. Lett. B **774**, 643 (2017).

[59] L. Bian, S. M. Choi, Y. J. Kang and H. M. Lee, Phys. Rev. D **96**, no. 7, 075038 (2017).

[60] P. Cox, C. Han and T. T. Yanagida, JCAP **1801**, no. 01, 029 (2018).

[61] P. del Amo Sanchez *et al.* [BaBar Collaboration], Phys. Rev. Lett. **104**, 191801 (2010).

[62] D. A. Faroughy, A. Greljo and J. F. Kamenik, Phys. Lett. B **764**, 126 (2017).

[63] M. Aaboud *et al.* [ATLAS Collaboration], JHEP **1801**, 055 (2018).

[64] E. J. Chun, A. Das, J. Kim and J. Kim, JHEP **1902**, 093 (2019).

[65] F. Elahi and A. Martin, Phys. Rev. D **100**, no. 3, 035016 (2019).

[66] T. Appelquist, B. A. Dobrescu and A. R. Hopper, Phys. Rev. D **68** 035012 (2003).

[67] S. Oda, N. Okada and D. s. Takahashi, Phys. Rev. D **92**, no. 1, 015026 (2015).

[68] A. Das, S. Oda, N. Okada and D. s. Takahashi, Phys. Rev. D **93** no.11, 115038 (2016).

[69] S. Jung, H. Murayama, A. Pierce and J. D. Wells, Phys. Rev. D **81**, 015004 (2010).

[70] N. Okada and O. Seto, Phys. Rev. D **98**, no. 6, 063532 (2018).

[71] W. Chao, W. F. Cui, H. K. Guo and J. Shu, Chin. Phys. C **44**, no.12, 123102 (2020)

[72] G. Jungman, M. Kamionkowski and K. Griest, Phys. Rept. **267**, 195 (1996).

[73] R. N. Mohapatra and N. Okada, Phys. Rev. D **107**, no.9, 095023 (2023).

[74] N. Aghanim *et al.* [Planck], Astron. Astrophys. **641**, A6 (2020) [erratum: Astron. Astrophys. **652**, C4 (2021)].

[75] [CMS], CMS-PAS-EXO-21-016.

[76] G. Aad *et al.* [ATLAS], Phys. Lett. B **796**, 68-87 (2019).

[77] J. Pumplin, D. R. Stump, J. Huston, H. L. Lai, P. M. Nadolsky and W. K. Tung, JHEP **07**,

012 (2002).

- [78] D. Curtin and M. E. Peskin, Phys. Rev. D **97**, no.1, 015006 (2018).
- [79] D. Curtin, K. Deshpande, O. Fischer and J. Zurita, JHEP **07**, 024 (2018).